TUNTWIN's Workshop

Session B: Spectroscopy techniques session

Funded by the Horizon 2020 Framework Programme of the European Union under the GA N° 952306

Session: Spectroscopy techniques

Synchrotron based infrared microspectroscopy

Iris H.Valido

Synchrotron based infrared microspectroscopy

- Introduction
- Why use synchrotron radiation?
- Examples
- Wrap-up

Synchrotron based infrared microspectroscopy

- **Introduction**
- Why use synchrotron radiation?
- Examples
- Wrap-up

Synchrotron based infrared microspectroscopy: Introduction

depts.washington.edu

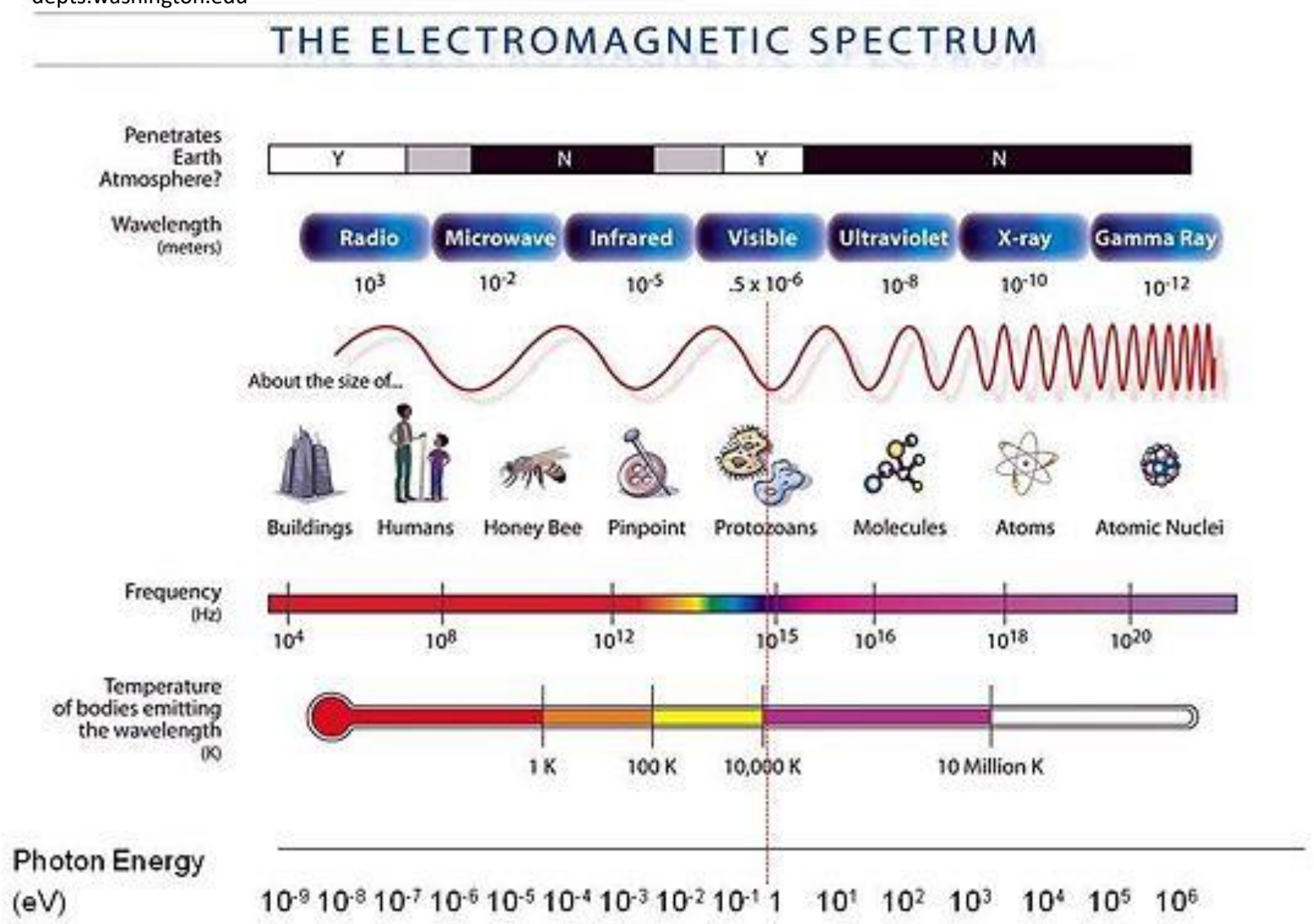

Synchrotron based infrared microspectroscopy: Introduction

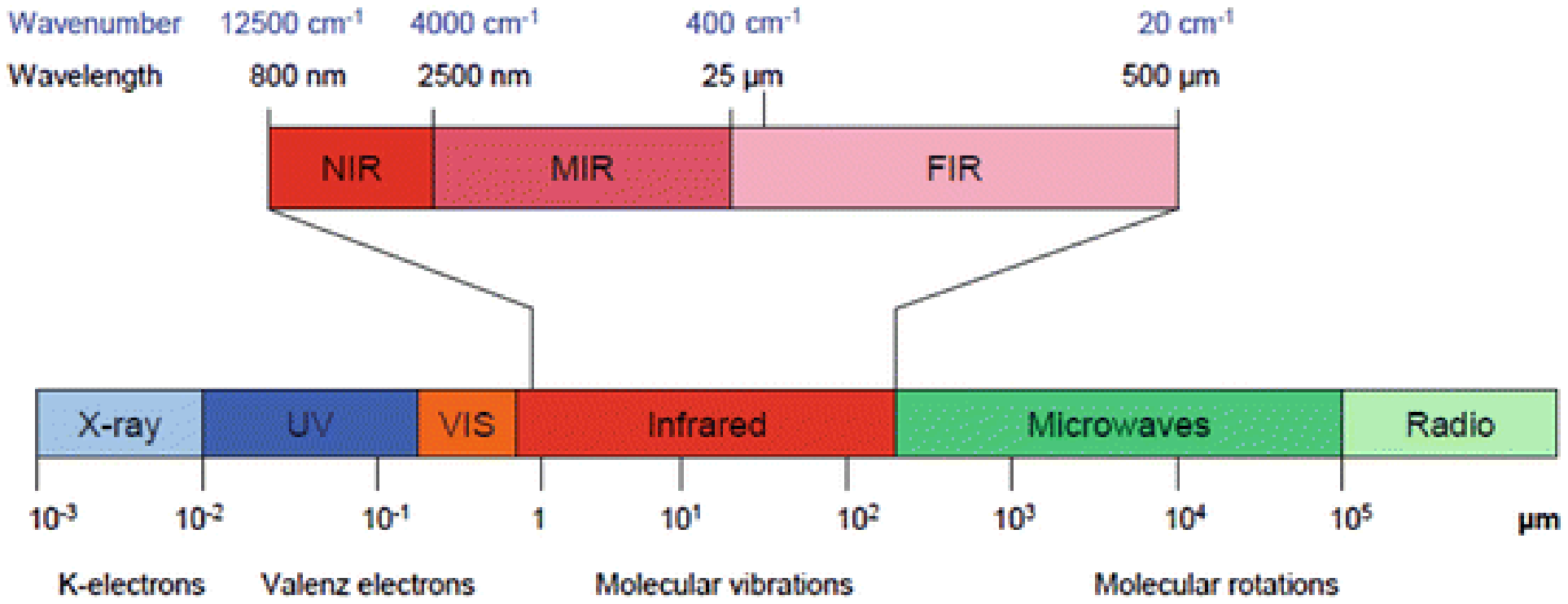

Reich, G. (2016). Mid and Near Infrared Spectroscopy. https://doi.org/10.1007/978-1-4939-4029-5_3

Synchrotron based infrared microspectroscopy: Introduction

The IR spectroscopic process

As a molecule vibrates, there is a fluctuation in its dipole moment (which is determined by the magnitude of the charge difference and the distance between the two centers of charge), this causes a field that interacts with the electric field associated with radiation.

A criterion for IR absorption is a net change in dipole moment in a molecule as it vibrates or rotates.

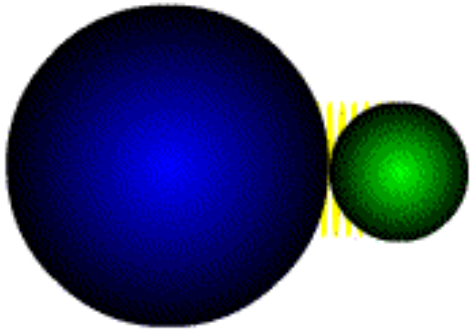

Vibration of a Diatomic Molecule
Approximates an Oscillating Spring

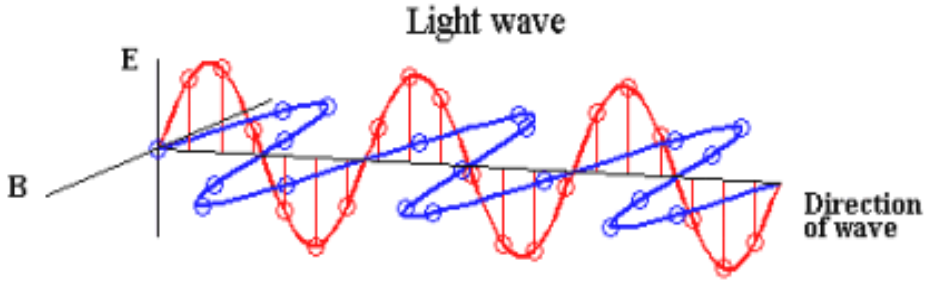

R. Osibanjo, R. Curtis and Z. Lai (2022). Infrared Spectroscopy. Chem.libretexts.org

Synchrotron based infrared microspectroscopy: Introduction

IR vibrational modes

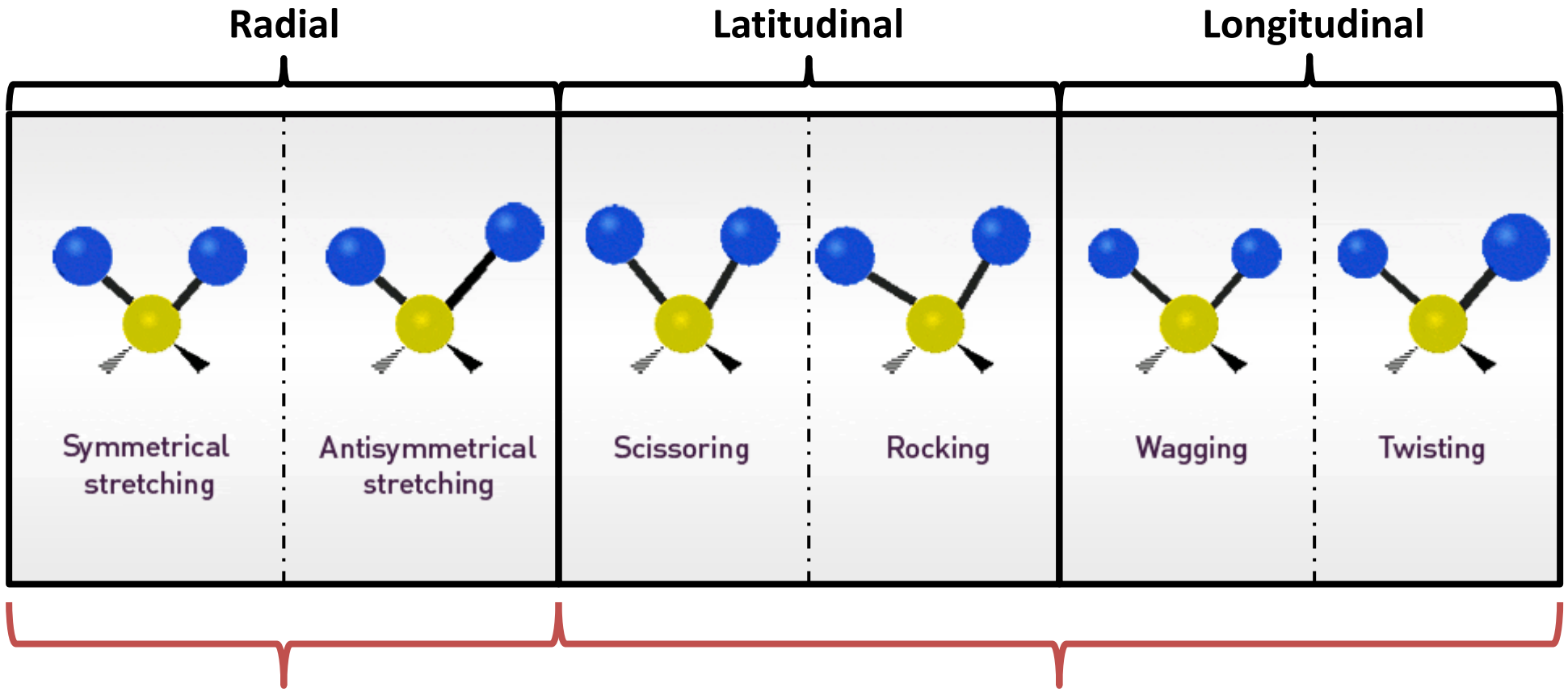

Synchrotron based infrared microspectroscopy: Introduction

Example: typical IR spectra of a biological sample

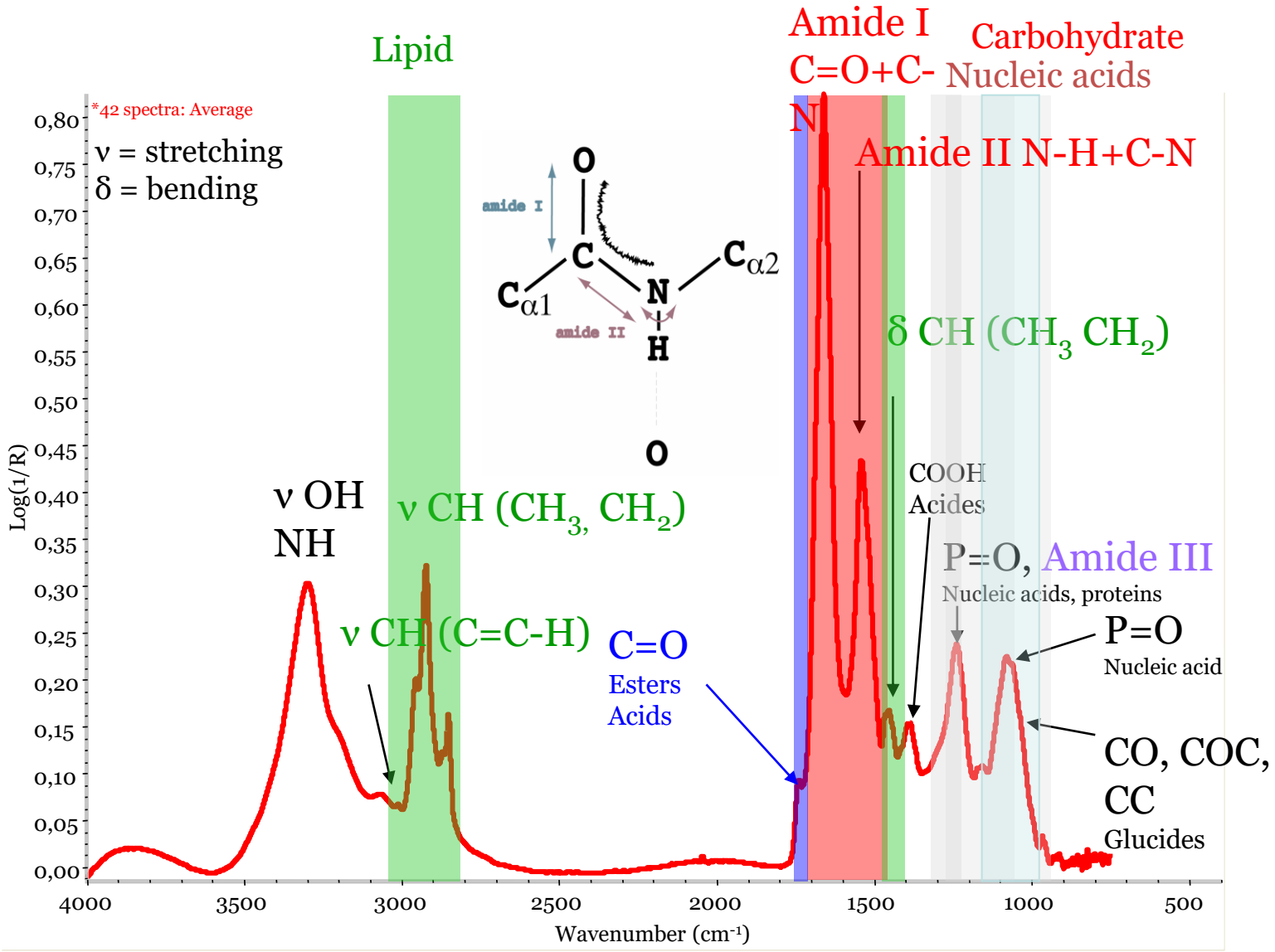

Synchrotron based infrared microspectroscopy

How to measure?

Synchrotron based infrared microspectroscopy: Introduction

How to measure?

Transmission

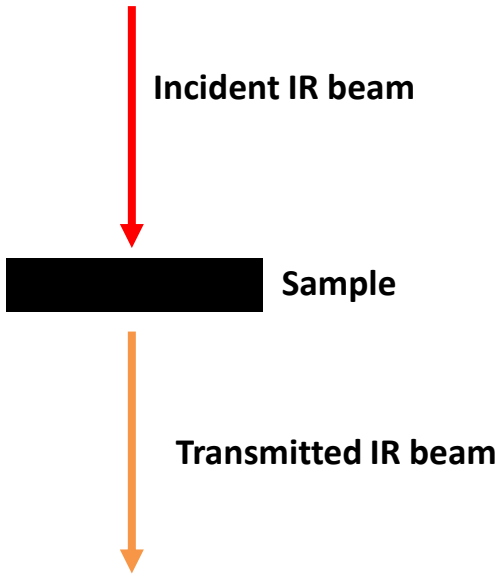

Reflection

Specular reflection

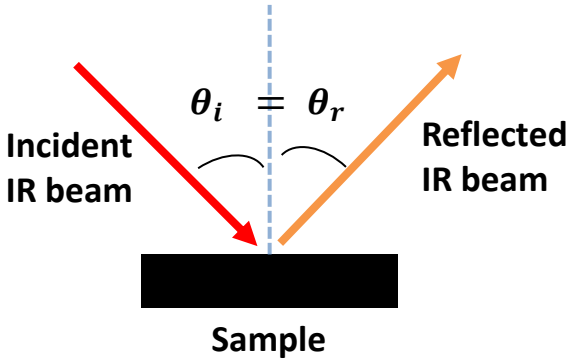

Diffuse reflection

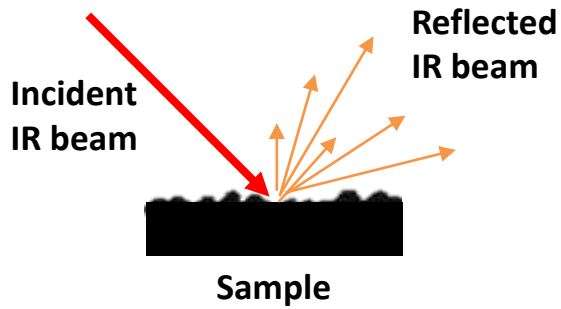

Reflection-absorption

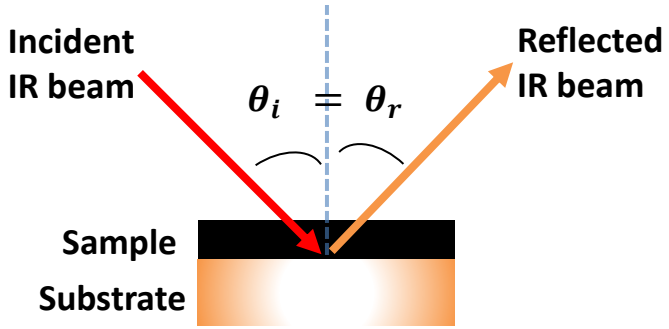

Attenuated total reflectance

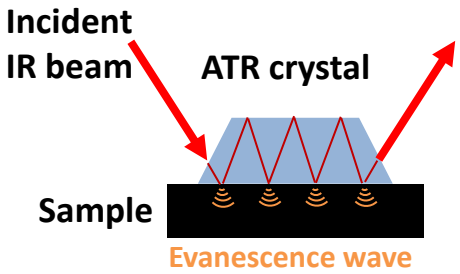

Synchrotron based infrared microspectroscopy

- Introduction
- **Why use synchrotron radiation?**
- Examples
- Wrap-up

Synchrotron based infrared microspectroscopy: Why synchrotron?

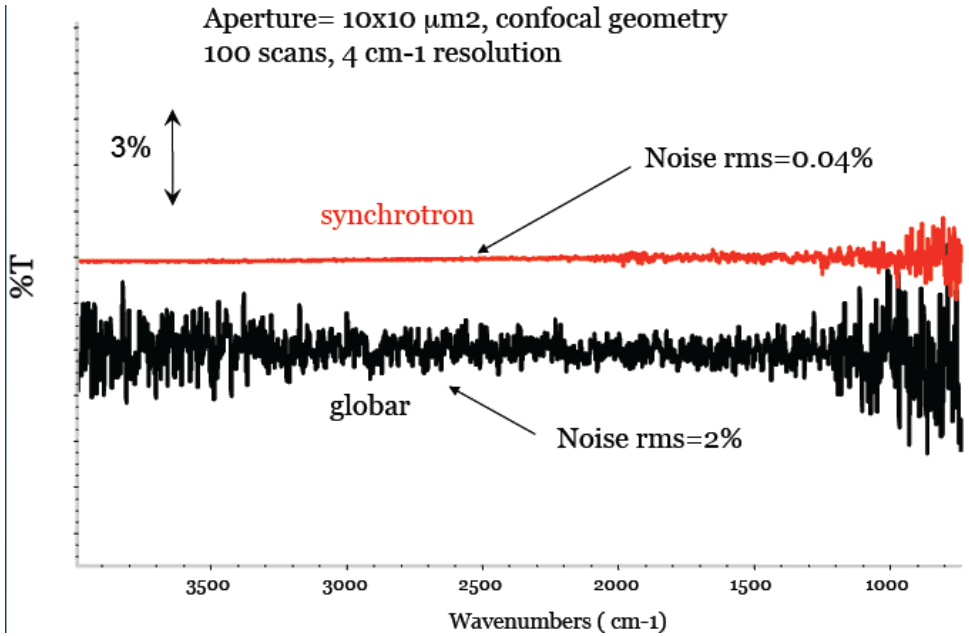

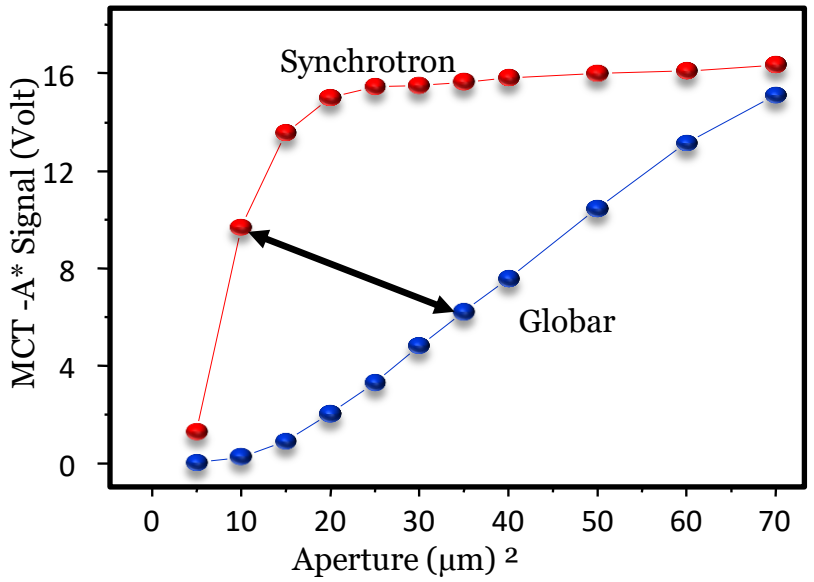

The synchrotron source achieves this performance by delivering up to 10^3 times more IR light onto a 3 µm spot than a conventional IR Globar source (black body radiation).

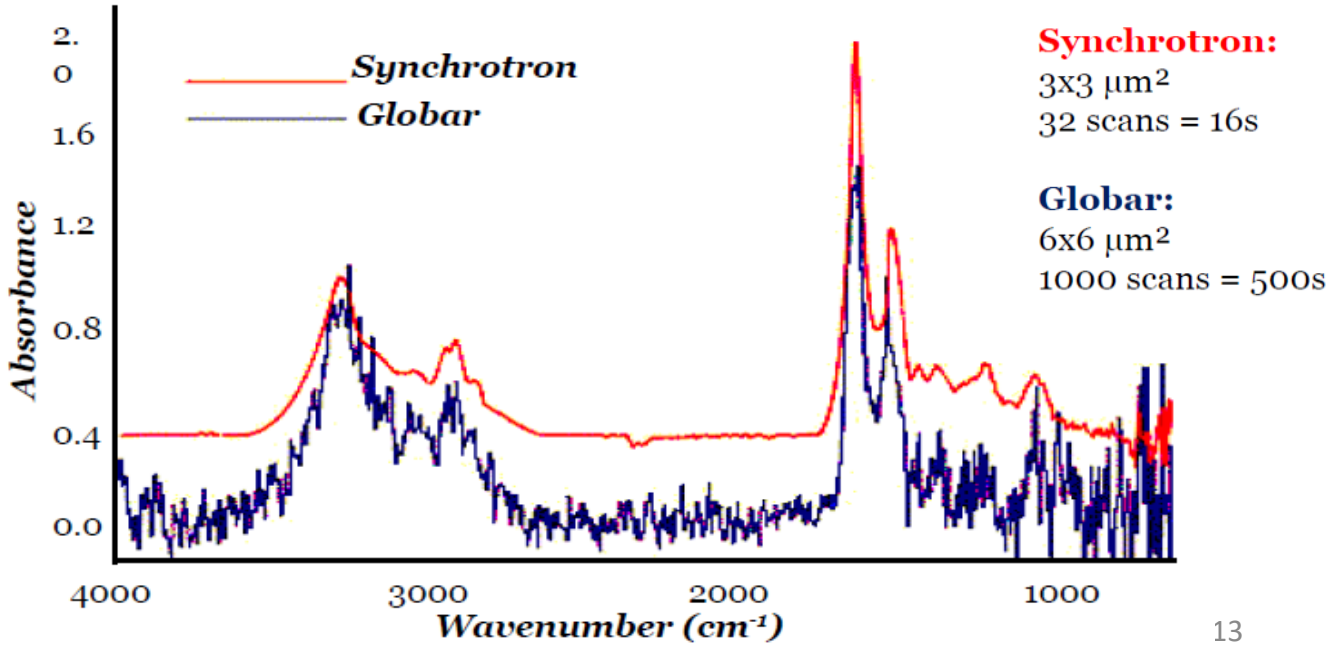

Courtesy of Dr. Ibraheem Yousef (Beamline responsible of MIRAS beamline at ALBA)

Synchrotron based infrared microspectroscopy: Softwares

OPUS

Matlab

Unscrambler
by Camo Analytics

Synchrotron based infrared microspectroscopy

- Introduction
- Why use synchrotron radiation?
- **Examples**
- Wrap-up

Synchrotron based infrared microspectroscopy: Examples

1. S, N-doped carbon dots-based cisplatin delivery system in adenocarcinoma cells: Spectroscopical and computational approach

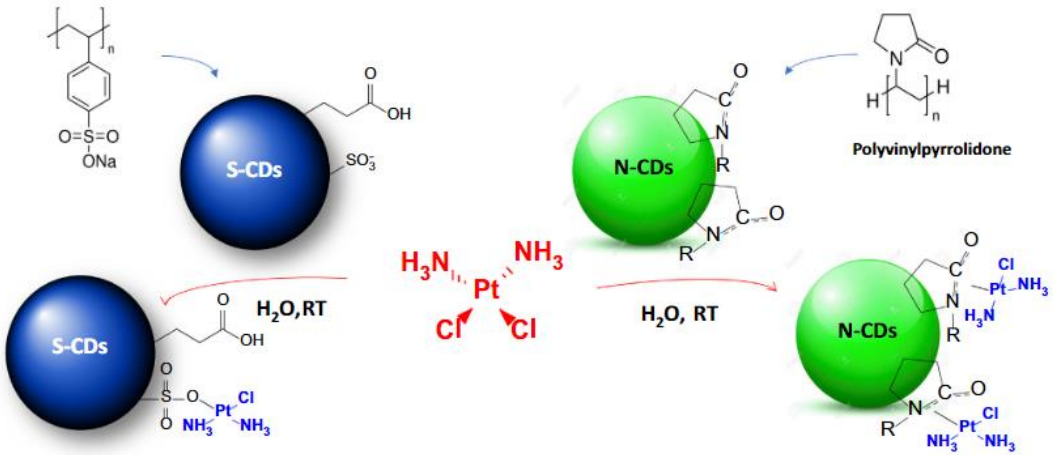

Fig. 3. Schematic representation of the surface functionalization of S-CDs@*cis*-Pt (left) and *N*-CDs@*cis*-Pt (right).

230

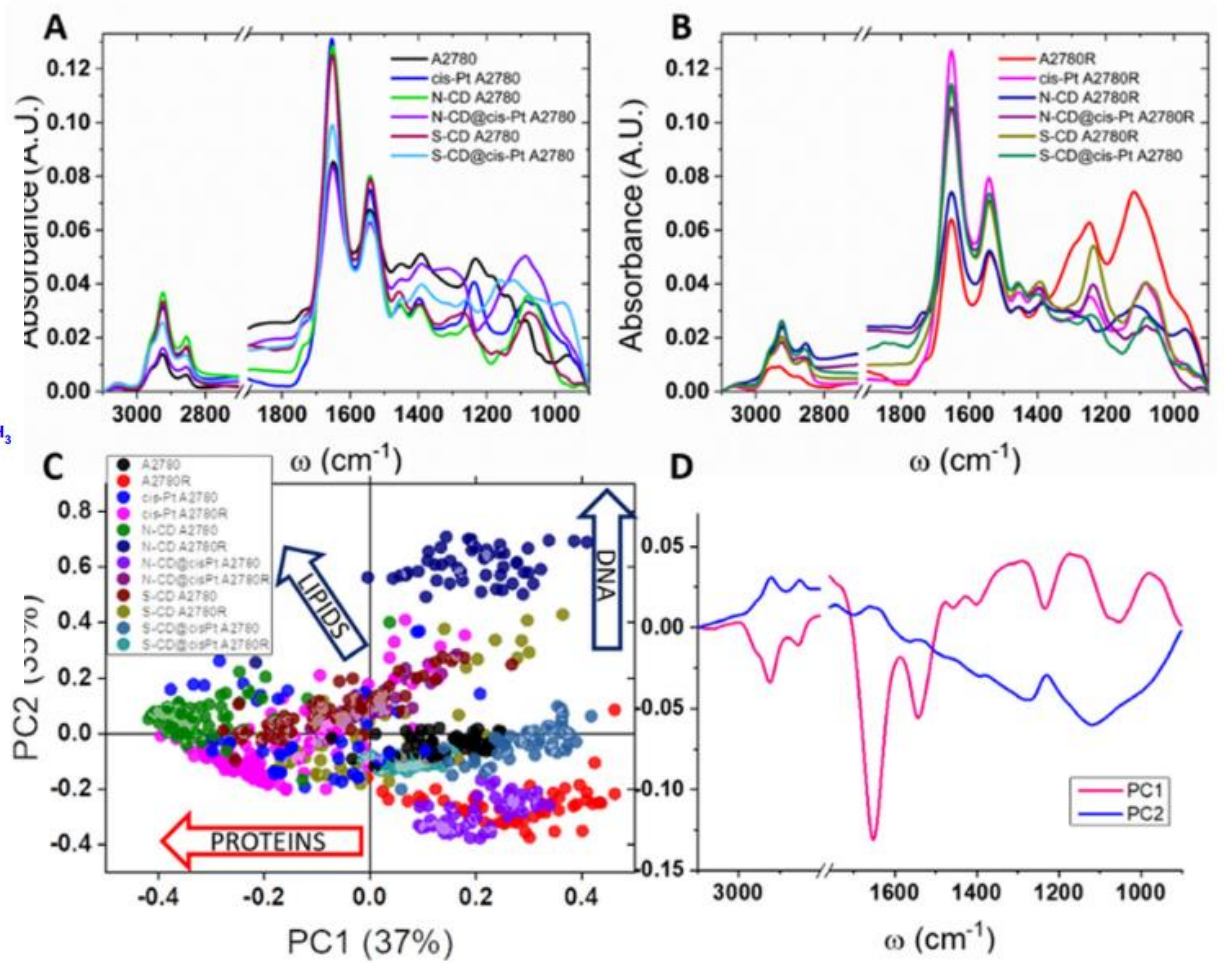

Fig. 6. (**A**) Averaged FTIR spectra of the sensitive and (**B**) *cis*-Pt resistant A2780 cells (**B**) untreated, *cis*-Pt-treated, *N*-CDs-treated, S-CDs-treated, and cells treated with *N*-CDs or S-CDs and *cis*-Pt simultaneously. Each treatment is indicated by a different color of spectra (N = 50). (**C**) The PCA score plot of two first PCA components and (**D**) contribution of individual absorbance to these components (loading plot).

T. Ducic, et al. Journal of Colloid and Interface Science 623 (2022) 226-237. doi.org/10.1016/j.jcis2022.05.005

Synchrotron based infrared microspectroscopy: Examples

2. Lipid Status of A2780 Ovarian Cancer Cells after Treatment with Ruthenium Complex Modified with Carbon Dot Nanocarriers: A Multimodal SR-FTIR Spectroscopy and MALDI TOF Mass Spectrometry Study

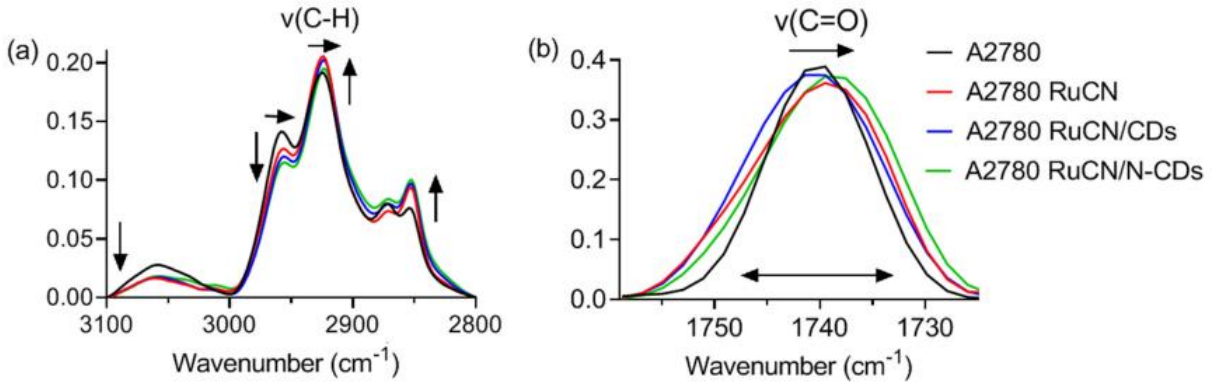

Figure 4. The lipid fingerprint area ((ν(C–H) (**a**) and ν(C=O) (**b**)) of the untreated A2780 cancer cells (black line) and cells treated with RuCN complex (red line), RuCN/N-CDs (green line), and RuCN/CDs (blue line).

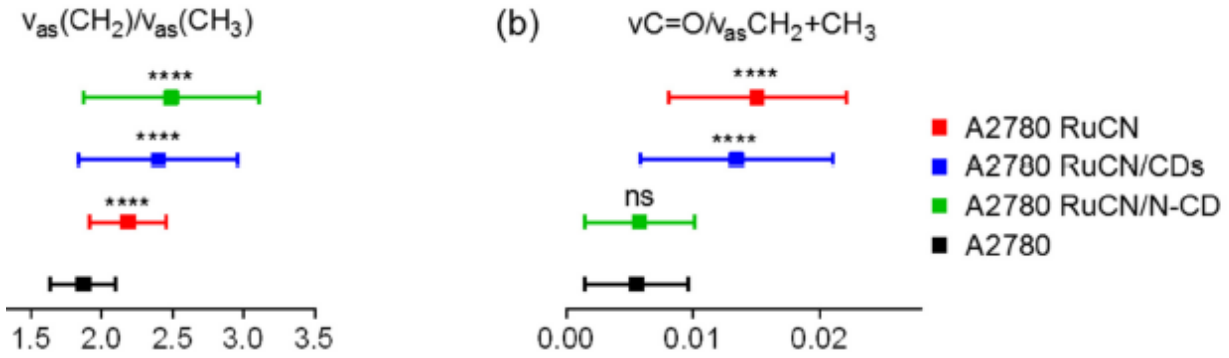

Figure 5. Analysis of oxidative stress markers. (**a**) Distribution of the ratios between asymmetric CH_2 and CH_3 bands ($\nu_{as}(CH_2)/\nu_{as}(CH_3)$). (**b**) Distribution of the ratio between the C=O band and the sum of asymmetric CH_3 and CH_2 bands ($\nu(C=O)/\nu_{as}(CH_2 + CH_3)$). Values are presented with the mean ± SD. All the values are compared to the control (A2780 untreated cells, black color). **** indicates values that are significantly different ($p \leq 0.0001$); ns, not significant ($p > 0.05$).

M. D. Nesic, et al. Cancers 2022, 14, 1182. doi.org/10.3390/cancers14051182

Synchrotron based infrared microspectroscopy: Examples

3. UV Effect on Human Anterior Lens Capsule Macro-Molecular Composition Studied by Synchrotron-Based FTIR Micro-Spectroscopy

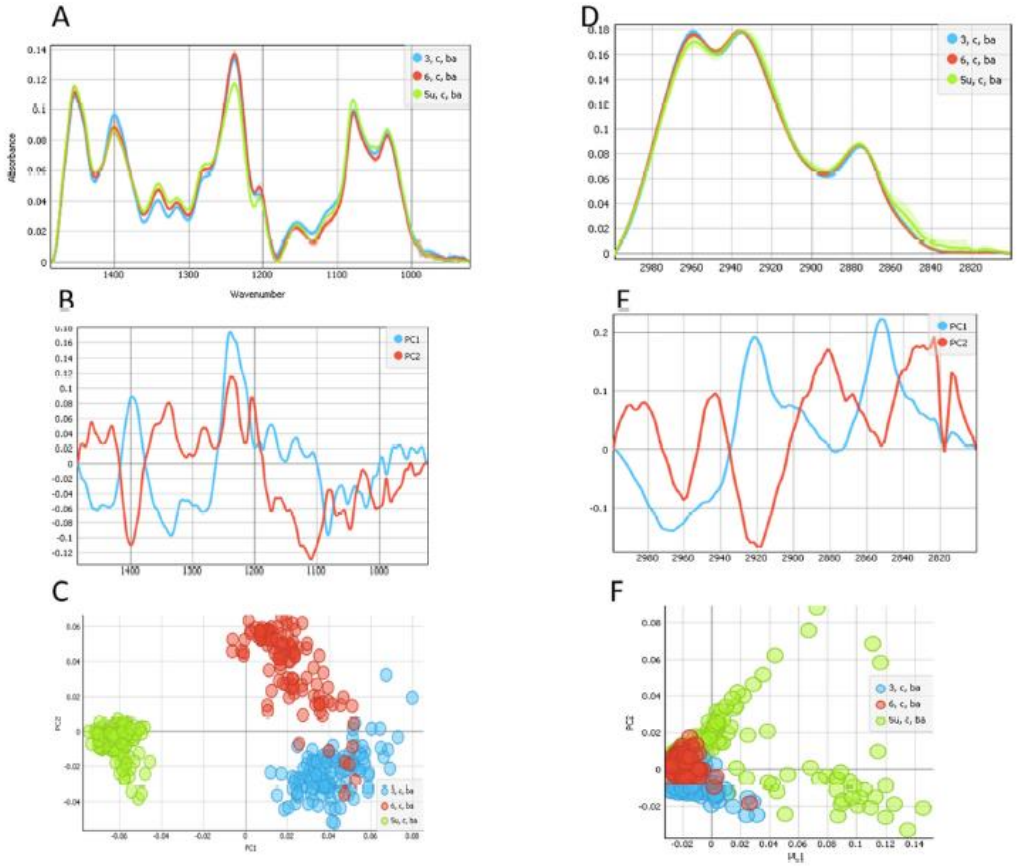

Figure 2. Analysis of the spectral region of the nucleic acids and carbohydrates (**A**–**C**) and lipids (**D**–**F**) of UV-irradiated (green) non-cataractous LC and the two non-irradiated (red and blue) non-cataractous LCs. (**A**) The FTIR average spectra of fingerprint area (950–1485 cm^{-1}). (**B**) The PCA score plot denotes the variability associated with the first two components. (**C**) First and second PCA components, PC1 and PC2 score plot. (**D**) The FTIR average spectra of lipid area (2800–3000 cm^{-1}). (**E**) The PCA score plot denotes the variability associated with the first two components. (**F**) First and second PCA components, PC1 and PC2 score plot.

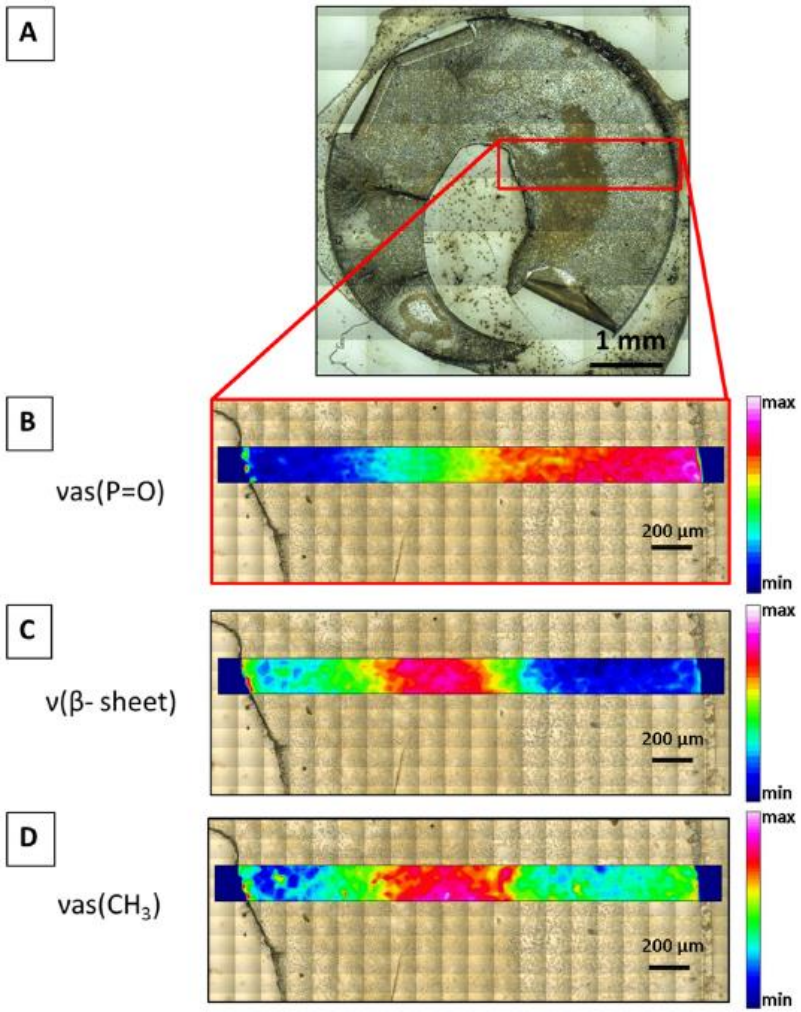

Figure 4. (**A**) Visible image of a non-cataractous LC 3, C, and Ba taken in reflection geometry. Highlighted is the FTIR imaging area. Visible images with higher magnification achieved in transmission geometry are shown below with overlapped chemical FTIR micro-spectroscopy images showing the integrated intensities of the vas (P=O) band at 1238 cm^{-1} (**B**), the β-sheet contribution at 1625 cm^{-1} (**C**), and the υ_{as} (CH_3) at 2960 cm^{-1} (**D**).

X. Lumi, et al. Int. J. Mol. Sci. 2021, 22, 5249. doi.org/10.3390/ijms22105249

Synchrotron based infrared microspectroscopy: Examples

4. Linear unmixing protocol for hyperspectral image fusion analysis applied to a case study of vegetal tissues

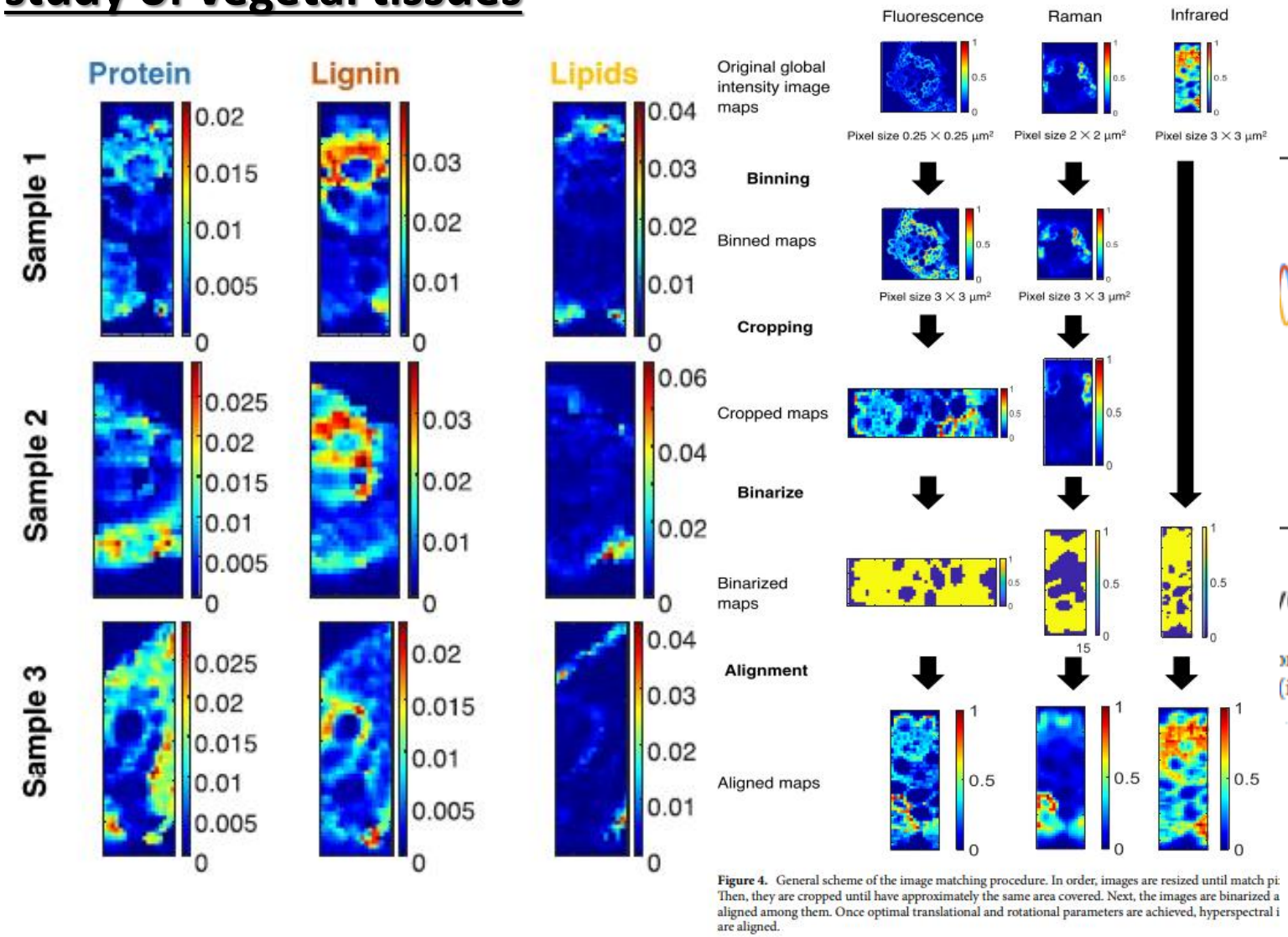

Figure 4. General scheme of the image matching procedure. In order, images are resized until match pi
Then, they are cropped until have approximately the same area covered. Next, the images are binarized a
aligned among them. Once optimal translational and rotational parameters are achieved, hyperspectral i
are aligned.

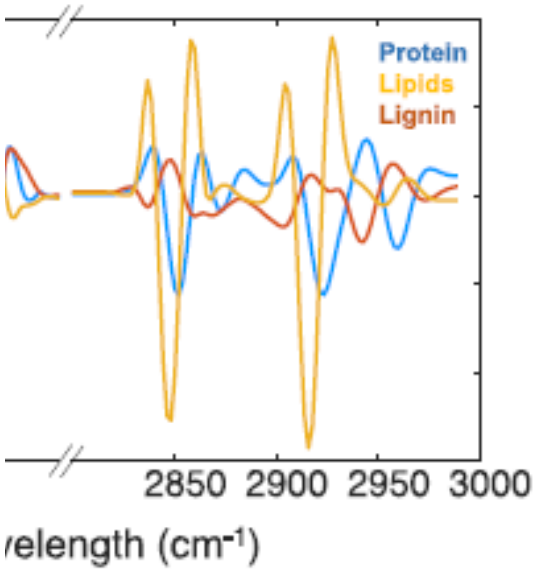

or the three components. Bottom plot, pure SR-FTIR spectral
(in yellow), to proteins (in blue) and lignin (orange).

A. Gomez-Sanchez, et al. Scientific Reports (2021) 11:18665. doi.org/10.1038/s41598-021-98000-0

Synchrotron based infrared microspectroscopy: Examples

5. Calcium oxalate kidney stones, where is the organic matter?: A synchrotron based infrared microspectroscopy study

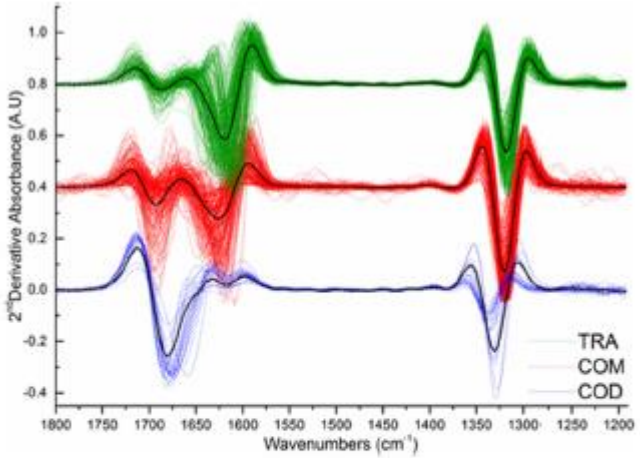

FIGURE 3 Second derivative spectra of the samples analyzed in the PCA (Figure 2) on the region between 1800 and 1190 cm^{-1}. Groups are divided in COD (blue-bottom), COM (red-middle), and TRA (green-top) according to the sample classification by morpho-constitutional analysis. The black lines represent the average of each group

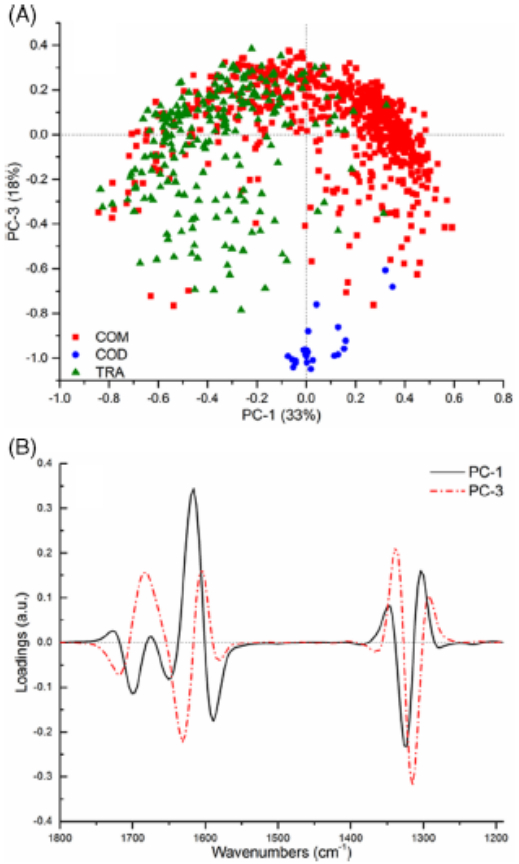

FIGURE 2 Principal component analysis (PCA) of the region between 1800 and 1190 cm^{-1} (unit vector normalization of the second derivative) corresponding to kidney stones samples previously classified as COM (red squares), COD (blue circles) and TRA (green triangles) by morpho-constitutional analysis: A, scores graph and B, PC-1 and PC-3 loadings of the PCA

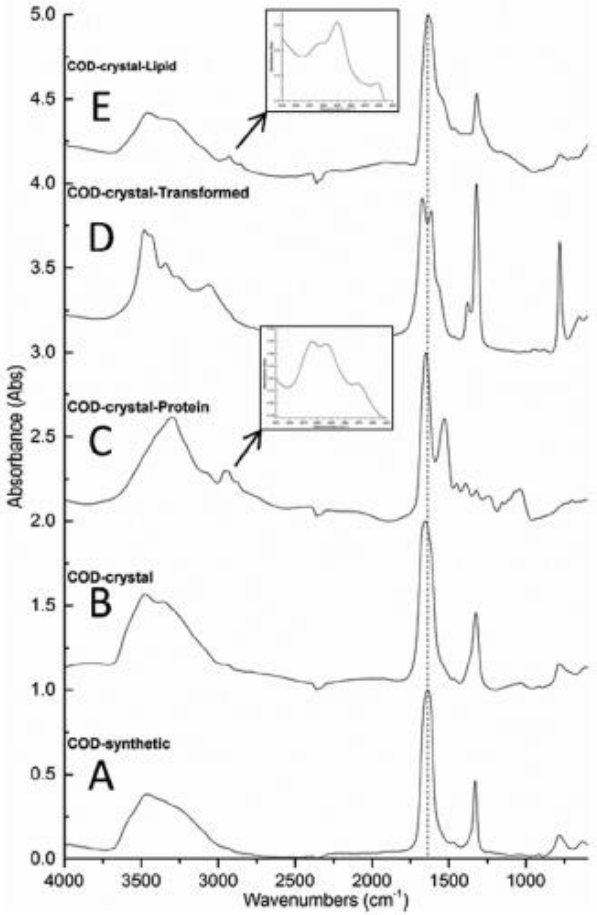

FIGURE 4 A, Examples of synchrotron FTIR spectra of synthetic COD; B, a typical crystal of COD; C, protein; and D, transformed COD; found in COD crystallites undergoing the transformation process, E, and of lipids found on a non-transformed COD crystal

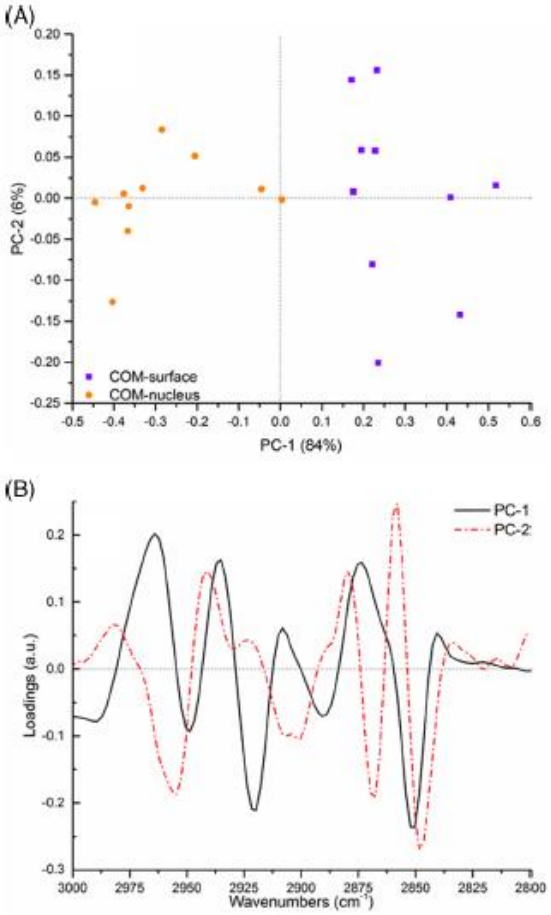

FIGURE 5 Principal Component Analysis (PCA) of the region between 3000-2800 cm^{-1} (unit vector normalization of the second derivative) corresponding to COM crystals selected from the nucleus (orange) and surface (purple) of a quiescent kidney stone: (A) scores graph and (B) PC-1 and PC-2 loadings of the PCA

I. H.Valido, et al. J. Biophotonics. 2020;e202000303. doi.org/10.1002/jbio.202000303

Synchrotron based infrared microspectroscopy: Examples

6. Tooth whitening, oxidation or reduction? Study of physicochemical alterations in bovine enamel using Synchrotron based Micro-FTIR

Vibration	$\nu_3\ PO_4^{3-}$	$\nu_1\ PO_4^{3-}$	$\nu_3\ CO_3^{2-}$		$\nu_2\ CO_3^{2-}$
Range (cm^{-1})	1160-965	965-935	1530-1550	1580-1320	880-830

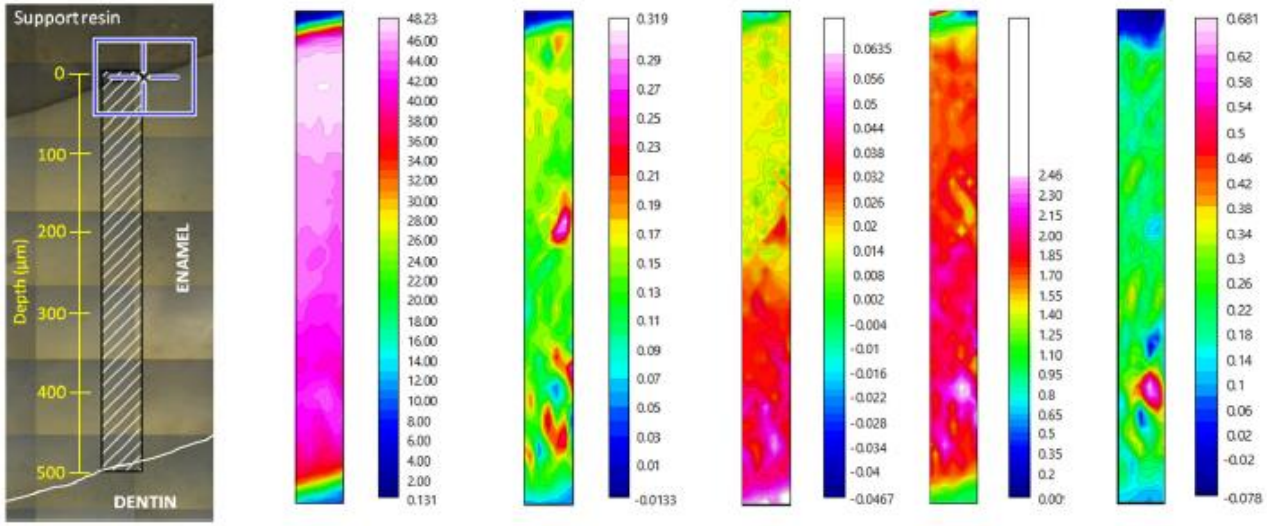

Fig. 2 – Chemical distribution (calculated by peak integration) of carbonates and phosphates in the middle crown of a bovine incisor control tooth (vertical section). The mappings where obtained using OPUS by performing chemical imaging, using peak integration mode A.

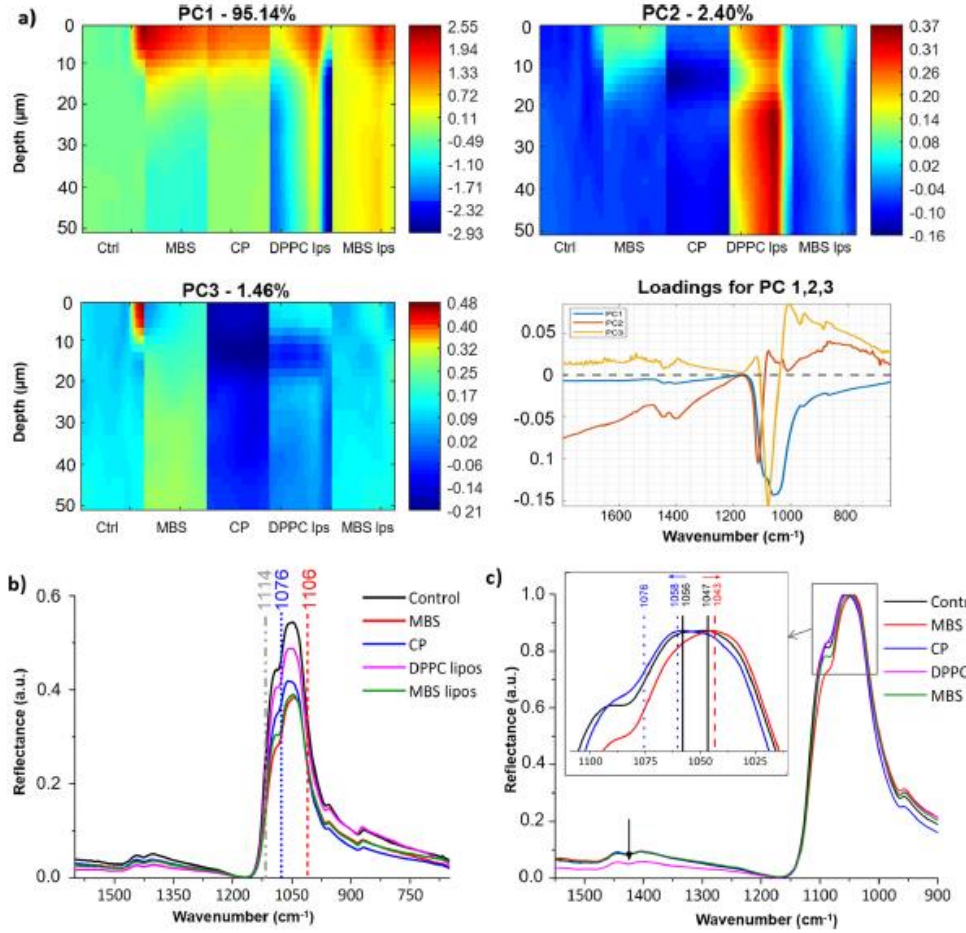

Fig. 4 – (a) Scores (distributed across the enamel depth, starting in the enamel surface at 0–50 µm deep), and loadings for the PCA treatments. (b) Average of the spectra corresponding to the first 10 µm for each treatment (n = 12). (c) Plot b normalized to maximum. Red dash line: MBS shift. Blue dots line, CP shift. Dash and dots grey line: characteristic shoulder of the HAP peak.

C. Babot-Marquillas, et al. Dental Materials 38 (2022) 670-679. doi.org/10.1016/j.dental.2022.02.006

Synchrotron based infrared microspectroscopy: Examples

7. Boron-Based Functional Additives Enable Solid Electrolyte Interphase Engineering in Calcium Metal Battery

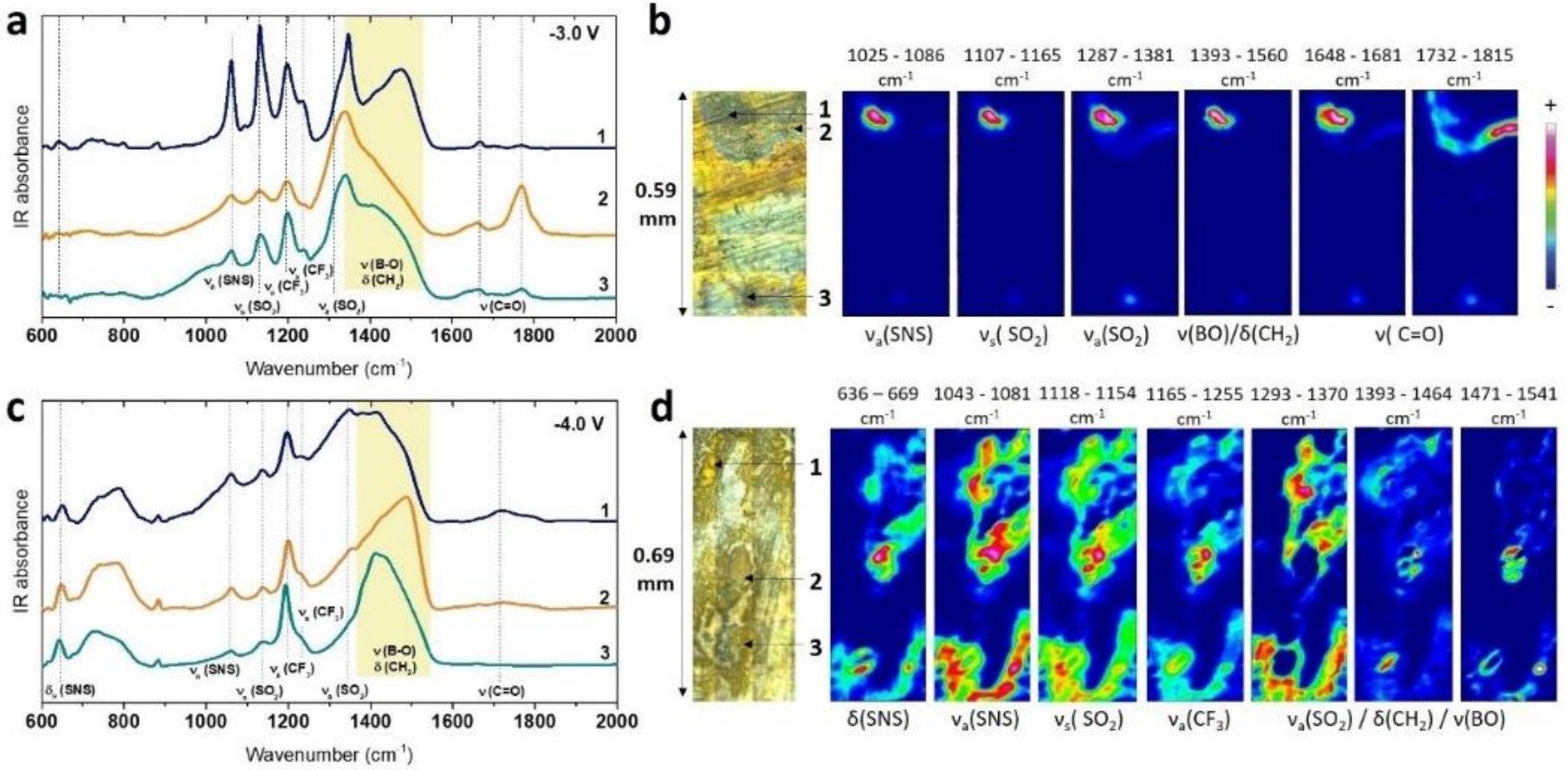

Figure 6. IR analysis of the SEI layers for the samples polarized during 48 h at a, b) −3.0 V and c, d) −4.0 V vs. Ag_{QRE}. a, c) FTIR-microspectroscopy spectra of the regions 1, 2, 3 marked on panels (b) and (d), dash lines are guides for the eye. b, d) Associated chemical images of the surface of the deposit for particular bands. The color scale corresponds to the intensity of the respective FTIR peak.

C. Bodin et al. Batteries& Supercaps2022,e202200433(1 of 13). doi.org/10.1002/batt.202200433

Synchrotron based infrared microspectroscopy: Examples

8. Pressure-Driven Symmetry-Preserving Phase Transitions in $Co(IO_3)_2$

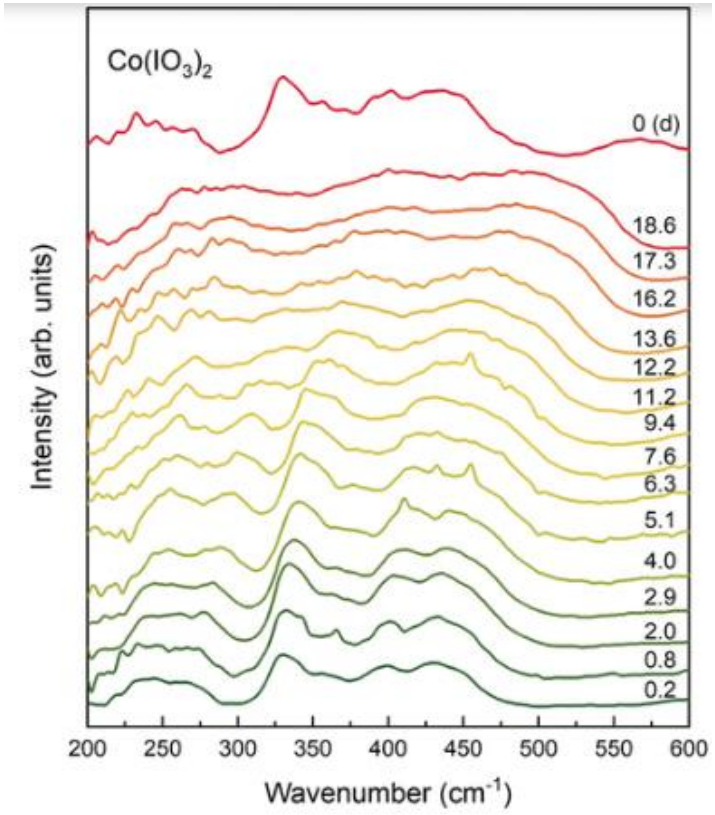

Figure 11. HP-FTIR spectra of $Co(IO_3)_2$ at selected pressures. The "d" in the top spectrum means that it is collected during the decompression process. The pressure of each pattern is shown on the right in "GPa".

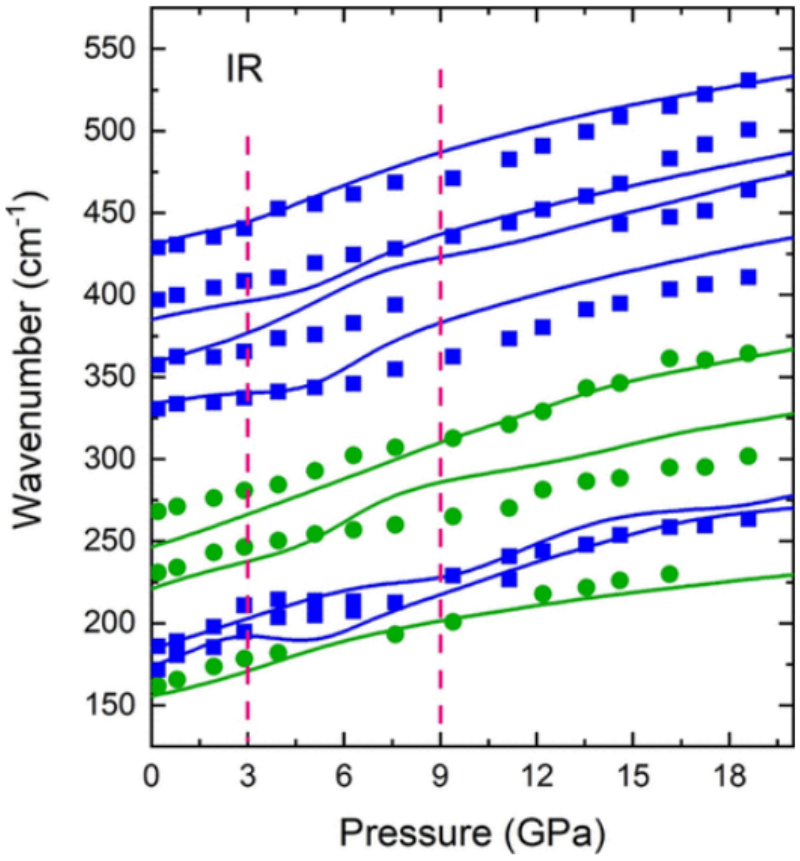

Figure 12. Pressure dependence of the IR-active wavenumbers in $Co(IO_3)_2$. Symbols correspond to experimental data while lines correspond to theoretically calculated data. A- and B-symmetries are represented by green and blue colors, respectively. Vertical pink dashed lines indicate suggested transition pressures. For the whole calculated IR-active modes in that region, the reader can find it in the Supporting Information, Figure S14.

A. Liang, et al. J. Phys. Chem. C 2021, 125, 31, 17448–17461. doi.org/10.1021/acs.jpcc.1c04659

Synchrotron based infrared microspectroscopy

- Introduction
- Why use synchrotron radiation?
- Examples
- **Wrap-up**

Synchrotron based infrared microspectroscopy: Wrap-up

Why use SR-µFTIR?

Advantages

- Simple
- Quick
- Non-destructive
- Sensitive
- Coupling with other techniques
- Flexible: solids, liquids, powders, thin films…

Applications

- Astrophysics
- Biology
- Plant biology
- Chemistry
- Geology
- Heritage Science
- Pharmaceutics
- Physics
- Polymers
- Surface sciences
- Environmental science

TUNTWIN's Workshop

شكرا

Merci!

Thank you!

¡Gracias!

CONTACT DETAILS:

Iris H.Valido

Postdoctoral Researcher

Chemistry Department, Science Faculty

Campus UAB, 08193, Bellaterra

Barcelona, Spain.

Email: iris.henriquez@uab.cat

Commission européenne

Funded by the Horizon 2020 Framework Programme of the European Union under the GA N° 952306

TUNTWIN